HOW ANTI-ALIASING FILTER AFFECTS IMAGE CONTRAST: AN ANALYSIS FROM MAJORIZATION THEORY PERSPECTIVE

Ketan Tang, Oscar C. Au, Lu Fang, Zhiding Yu, Yuanfang Guo *

Department of Electronic and Computer Engineering
Hong Kong University of Science and Technology
Hong Kong SAR, China
{tkt, eeau, fanglu, zdyu, eeandyguo}@ust.hk

ABSTRACT

When we design an anti-aliasing low pass filter, it is usually an IIR filter. We need to truncate the filter to an FIR filter. One may think that the more taps there are, the better the image quality is. However, we find that there exists an optimal value of tap number that will give the best visual quality. Filters with larger or smaller number of taps will degrade the image quality, due to the fact that the image contrast is reduced. In this paper we analyze this phenomenon using majorization theory and find that the image contrast can be formulated as a Schur convex function on filter coefficients. We also propose an effective method to choose the best filter so that the image contrast is maximized, so as to give best visual quality.

***Index Terms*—** anti-aliasing filter, contrast, majorization theory, Schur convex

1. INTRODUCTION

In the context of image downsampling, usually we need to filter the image using a low pass filter before downsampling it, otherwise there will be severe aliasing artifact. The most commonly used anti-aliasing filters are bilinear or bicubic filter ([6]). However, a better way of anti-aliasing filtering is to design a filter in frequency domain, and then transform it into spatial domain ([7, 8]). With the development of subpixel based rendering, new anti-aliasing filter for those subpixel downsampling is even more desired. Some traditional anti-aliasing filters may not be optimal for subpixel based downsampling, because subpixel based downsampling has different characteristics.

Take Diagonal Direct Subpixel based Downsampling method (DDSD) for example. As shown in Fig.1, we take R, G, B component from the three diagonal pixels respectively. The luminance spectrum for DDSD is shown in Fig.2 left. We can design a best elliptical low pass filter in frequency domain, as shown in Fig.2 right. This filter includes as much middle Y component, while excludes as much other information, as possible.

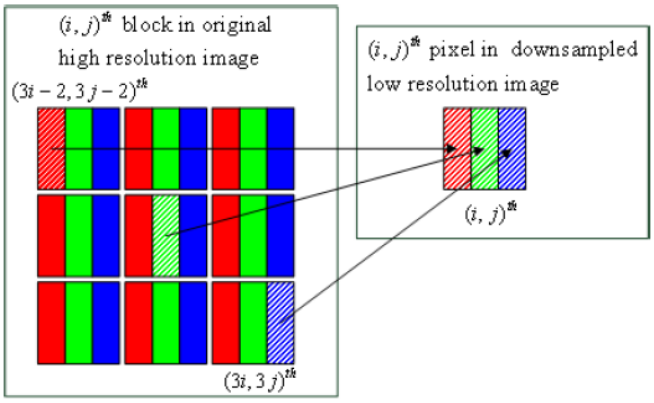

Fig. 1: DDSD paradigm.

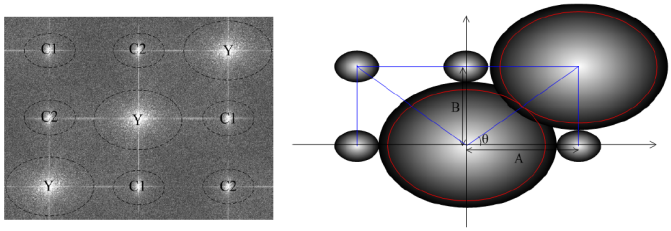

Fig. 2: DDSD spectrum (left) and corresponding anti-aliasing filter (right)

The next step is to transform this filter into spatial domain. Since the filter is usually Infinite Impulse Response (IIR) filter, it has to be truncated to get an approximated Finite Impulse Response (FIR) filter. The question is, how many taps shall we choose when truncating the IIR filter? One way is to randomly choose certain number of taps that is sufficient, or choose a small number of taps if computational complexity is a concern. However we find that, the tap number affects the visual quality of downsampled image quite a lot. And contrary to common belief, it is not that the more taps there are,

*This work has been supported in part by the Research Grants Council (RGC) of the Hong Kong Special Administrative Region, China. (GRF 610109).

978-1-61284-350-6/11/$26.00 ©2011 IEEE

(a) f_3, contrast=2782 (b) f_4, contrast=**2967** (c) f_5, contrast=2525

Fig. 3: Downsampled Cathedral image using DDSD with different tap numbers. The difference can be better observed on color screen. For FORG, filter h_4 also gives the best quality. Here due to space limitation we only show the FDDSD images ([**?**]).

(a) f_3', contrast=2782 (b) f_4', contrast=**2967** (c) f_5', contrast=2525

Fig. 4: The text region of DDSD downsampled Cathedral image with different tap numbers.

the better the quality is.

For the ease of representation, we denote by FDDSD the DDSD image with prefiltering, FORG the original size image with prefiltering, h_n the filter with $(2n+1)(2n+1)$ coefficients. Here h_n is a 2-D square filter and n is like a radius. And we denote by f_n the output image filtered by h_n. Fig.3 is an example of FDDSD with different tap numbers. We can see that f_4 has the best perceptual quality. However, the values of sharpness or aliasing effect of the three images are quite similar to each other. The good quality is mainly because that image f_4 has the highest contrast, especially in complex regions, e.g. the text region on the top right corner of image in Fig.4. If other measures (e.g. sharpness and aliasing effect) are similar for all three images, then the one with the larger contrast gives the better visual quality. In [9] the authors also found that human eyes are quite sensitive to image contrast. From Fig.3 we can see that f_4 has best visual quality and f_5 has the worst, which is consistent with their contrast values. The question is, why does filter h_4 give the best quality? Is there any truth behind this phenomenon? We will try to answer these questions in the following sections of this paper.

The rest of the paper is organized as follows. In section 2 we give a theoretical analysis of the relation between image contrast and filter coefficient using majorization theory. In section 3 we show some experimental results. And section 4 concludes this paper.

2. RELATION BETWEEN IMAGE CONTRAST AND FILTER COEFFICIENTS

We use the variance of luminance values as the contrast measure ([1, 9]), i.e. the contrast of an image is

$$Con = \text{Var}(I) = \text{E}(I_x - \bar{I})^2 = \frac{1}{N}\sum_x (I_x - \bar{I})^2 \quad (1)$$

where I_x is the luminance value at location x, $\bar{I}$ is the mean value of all I_x, and N is the total number of pixels in the image. We test tens of images and find that it is true all examples with highest contrast do have best visual quality. For the images shown in Fig.3 we list the contrast values. It is clearly shown that the images with largest contrast indeed have best visual quality.

Rewrite the contrast equation 1 as

$$Con = \text{E}(I_x^2) - \bar{I}^2 = \frac{1}{N}\sum_x I_x^2 - \bar{I}^2. \triangleq En - \bar{I}^2 \quad (2)$$

We see that what really matters is the average energy En, i.e. the mean square luminance value. Analyzing the contrast of FDDSD image is difficult. Fortunately, the contrast of FORG image is a good estimation.

Proposition 1: FDDSD has similar contrast of FORG image, assuming an image is a piecewise stationary random process.

It is not difficult to understand this proposition. Under the assumption of piecewise stationarity ([5]), the pixel values do not change much in a small region, thus the variance of original signal equals the variance of a uniformly subsampled version. But since we do not have infinite number of samples, equality is not guaranteed. We can only say the two contrasts are similar. And the piecewise stationarity assumption is reasonable for most images. From Table.1 we can see that indeed FORG image and FDDSD image have similar contrast.

Suppose the original non-filtered luminance image is L, the 2-D filter h_n is represented by a $m^2 \times 1$ $(m = (2n+1))$ vector c, and the luminance of FORG image is I. For a pixel

Table 1: FDDSD and FORG of "tree" image have similar contrast for all filters. Bold face numbers denote the best tap number.

ntap	1	2	3	4	5	6	7
Con_{FORG}	2709	2640	2905	**3139**	2774	2700	2847
Con_{FDDSD}	2660	2606	2833	**3030**	2710	2644	2774
$\frac{Con_{FORG}-Con_{FDDSD}}{Con_{FORG}}$	0.018	0.013	0.025	0.035	0.023	0.021	0.026

x, denote by b_x the vector form of the $m \times m$ neighbors of pixel x. We write the average energy in matrix form:

$$\begin{aligned} En &= \frac{1}{N}\sum_x I_x^2 = \frac{1}{N}\sum_x (c^T b_x)^2 \\ &= \frac{1}{N}\sum_x c^T b_x b_x^T c = c^T(\frac{1}{N}\sum_x b_x b_x^T)c \\ &\triangleq c^T R c \\ &= \text{Tr}(c^T R c) = \text{Tr}(Rcc^T) \triangleq \text{Tr}(RC) \end{aligned} \quad (3)$$

where $R = \frac{1}{N}\sum_x b_x b_x^T$ is the autocorrelation matrix, $C = cc^T$.

Since $\text{Tr}(RC)$ is a kind of inner product, it satisfies Cauchy-Schwarz inequality:

$$\begin{aligned} \text{Tr}(RC) &\leq \text{Tr}(R)\text{Tr}(C) = \sum_i R_{ii}\sum_i C_{ii} \\ &= (\frac{1}{N}\sum_i L_i^2)(\sum_i c_i^2) \end{aligned} \quad (4)$$

The first term on the right hand side is fixed for all filters, what matters is the second term $\sum_i c_i^2$, which is defined as Total Coefficient Energy (TCE) of the filter. Eq.4 actually gives an upper bound of average energy En. So a reasonable guess is, the larger TCE is, the larger En and Con is.

Indeed we test all images and find that the filter with largest TCE provides the best visual quality. For the picture "tree", Table.2 gives the total coefficient energy TCE and corresponding contrast value Con of FDDSD for tap number ntap=$0, \ldots, 7$, where ntap=0 means no filtering. Although Eq.4 only gives an upper bound, at least we know that the contrast is related to TCE. And from Table.2 we find that Con and TCE follow the same trend in general, i.e. the filter that gives larger TCE also gives larger Con. The only exception is when ntap=1 and ntap=6. However the deviation is very small. In general we still can accept the assumption that Con and TCE have same trend.

To get the precise evaluation of En, we need to make use of the structure of the autocorrelation model. We follow the commonly used circular model to assume that the correlation between two samples is calculated as ([3])

$$E[I_{k,l} \cdot I_{p,q}] = V(I)\rho^{\sqrt{(k-p)^2+(l-q)^2}} \quad (5)$$

Table 2: TCE and contrast values with different tap numbers for "tree" picture. Bold face numbers denote the best tap number.

ntap	0	1	2	3	4	5	6	7
TCE	1	0.1159	0.0737	0.1680	**0.2654**	0.1472	0.1207	0.1601
Con	3213	2660	2606	2833	**3030**	2710	2644	2774

where $V(I)$ is the variance of I. Since $V(I)$ is constant for a given image, in the following we will omit it and only consider the factor $\rho^{\sqrt{(k-p)^2+(l-q)^2}}$. Consider the 3×3 neighborhood, in which case R is a 9×9 matrix:

$$R = \begin{bmatrix} 1 & \rho & \rho^2 & \rho & \rho^{\sqrt{2}} & \rho^{\sqrt{5}} & \rho^2 & \rho^{\sqrt{5}} & \rho^{2\sqrt{2}} \\ \rho & 1 & \rho & \rho^{\sqrt{2}} & \rho & \rho^{\sqrt{2}} & \rho^{\sqrt{5}} & \rho^2 & \rho^{\sqrt{5}} \\ \rho^2 & \rho & 1 & \rho^{\sqrt{5}} & \rho^{\sqrt{2}} & \rho & \rho^{2\sqrt{2}} & \rho^{\sqrt{5}} & \rho^2 \\ \rho & \rho^{\sqrt{2}} & \rho^{\sqrt{5}} & 1 & \rho & \rho^2 & \rho & \rho^{\sqrt{2}} & \rho^{\sqrt{5}} \\ \rho^{\sqrt{2}} & \rho & \rho^{\sqrt{2}} & \rho & 1 & \rho & \rho^{\sqrt{2}} & \rho & \rho^{\sqrt{2}} \\ \rho^{\sqrt{5}} & \rho^{\sqrt{2}} & \rho & \rho^2 & \rho & 1 & \rho^{\sqrt{5}} & \rho^{\sqrt{2}} & \rho \\ \rho^2 & \rho^{\sqrt{5}} & \rho^{2\sqrt{2}} & \rho & \rho^{\sqrt{2}} & \rho^{\sqrt{5}} & 1 & \rho & \rho^2 \\ \rho^{\sqrt{5}} & \rho^2 & \rho^{\sqrt{5}} & \rho^{\sqrt{2}} & \rho & \rho^{\sqrt{2}} & \rho & 1 & \rho \\ \rho^{2\sqrt{2}} & \rho^{\sqrt{5}} & \rho^2 & \rho^{\sqrt{5}} & \rho^{\sqrt{2}} & \rho & \rho^2 & \rho & 1 \end{bmatrix}$$

Proposition 2: The function $En = c^T R c$ is a **Schur convex** function on c.

It is difficult to prove this proposition in general case. We only show the proof in 3×3 neighborhood case in the appendix. Note that for a general positive semi-definite matrix R, $c^T R c$ may not be a Schur convex function on c. But for a autocorrelation matrix R obtained from Eq.5 and a symmetric 2-D filter h, $c^T R c$ is a Schur convex function on c (c is the vector representation of h).

Since En is a Schur convex function on c, the concentrated c is, the larger En is. To measure the concentration of a vector c, we need to refer to **Majorization theory** ([2]). If two vectors x and y with length m satisfy $\sum_{i=1}^m x_i = \sum_{i=1}^m y_i$; $\sum_{i=1}^k x_{[i]} \leq \sum_{i=1}^k y_{[i]}$, $\forall k = 1, \ldots m$, where $x_{[i]}$ is the i-th largest element of x, we say x is majorized by y, or equivalently y majorizes x. In our work, since all filters are normalized to prevent DC drift:

$$h(i,j) = \frac{\tilde{h}(i,j)}{\sum_{i,j}\tilde{h}(i,j)}, \quad (6)$$

where $\tilde{h}$ is the filter vector before normalization. The constraint $\sum_{i=1}^m x_i = \sum_{i=1}^m y_i$ is naturally satisfied.

Now the goal is to find the filter that majorizes all other filters. And we find that h_4 majorizes all other filter coefficients except h_7, but h_7 does not majorize h_4 either. Fig.5 shows that h_4 majorizes h_3. Note that when comparing two vectors

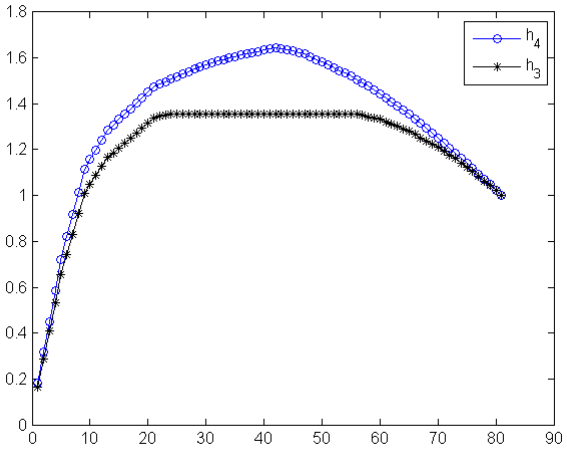

Fig. 5: h_4 majorizes h_3. x axis: k; y axis: $\sum_{i=1}^{k} h_{[i]}$

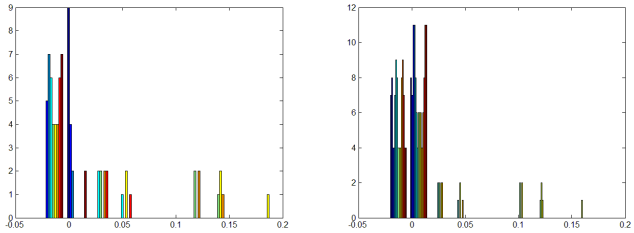

(a) h_4 (b) h_7

Fig. 6: Histogram plot of h_4 and h_7. We can see that h_4 is more concentrated than h_7.

with different length using majorization, the shorter vector needs to be padded zeros so that they have same length.

The reason why h_4 does not majorize h_7 and h_7 does not majorize h_4 is that, majorization is just a partial ordering and not all vectors can be compared by majorization. Nevertheless, h_4 is indeed more concentrated than h_7, which can be seen through the histogram plot in Fig.6. So we need to find a better measure of concentration.

Proposition 3: The function $\text{TCE}(c) = \sum_i c_i^2$ is a **Schur convex** function on c. En and TCE follow the same trend.

From Corollary 2.5 of [2] we know that $\phi(x) = \sum_i g(x_i)$ is Schur convex on x if $g(x_i)$ is convex on x_i, so TCE is Schur convex since each c_i^2 is convex on c_i. The second part of this proposition says that if $\text{TCE}(c_1) > \text{TCE}(c_2)$, then $En(c_1) > En(c_2)$. This part has not been proved, but through experiment we find it is true for a large amount of test images.

So instead of using the majorization definition above, we can use TCE to measure the concentration. TCE is also a Schur convex function on c, which means using TCE is enough to replace majorization relation to find the optimal filter. The strength of TCE is that, it is a total order. Any two filters can be compared using TCE.

To understand why h_4 gives the best result, we plot the 1-D profile of the middle row of the 2-D filter h_9 in Fig.7. We can see that, since $\tilde{h}(\pm 3, 0), \tilde{h}(\pm 4, 0)$ are negative, including the two will make the sum $\sum_{i,j} \tilde{h}(i,j)$ smaller, thus make the amplitude of each $h(i,0)$ larger. However, including $\tilde{h}(\pm 5, 0), \tilde{h}(\pm 6, 0)$ etc will make the amplitude of each $h(i,0)$ smaller. So for this particular case, h_4 gives the largest TCE.

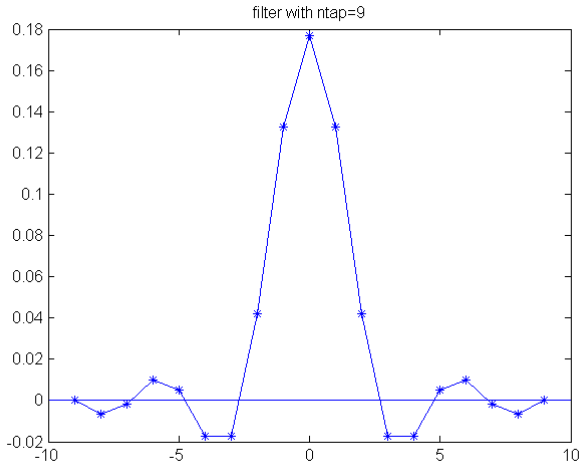

Fig. 7: 1-D profile of $h_9(\cdot, 0)$

Fig. 8: Test image examples.

3. EXPERIMENT RESULTS

To verify our discovery, we test tens of images, including natural images, synthesized images, high definition images, etc. Fig.8 shows some of our test images. For an input image, we design a low pass filter in frequency domain according to the shape of the luminance spectrum and Nyquist theorem, as shown in Fig.2. Then do inverse Fourier transform to get the IIR filter in spatial domain. Truncating the IIR filter with different tap numbers we get different approximated FIR filters h_n. To show that the influence of filter tap number on visual quality does not only happen with DDSD scheme, we also downsample the input image using DSD ([4]) and conventional Pixel-based Downsampling (PD) methods. Table.3 shows the TCE values for all filters and Table.4 shows the corresponding contrast values. We can see that the filter with largest TCE always gives highest contrast, thus gives the best visual quality.

From Table.4 we can also see that Con_3 and Con_7 is quite similar to Con_4 for all images, which is consistent with our observation that f_3 and f_7 have similar visual quality as f_4. This means that if computational complexity is a concern, h_3 is a good substitute to h_4.

4. CONCLUSION

In this paper we demonstrate an interesting phenomenon in anti-aliasing filter design, that is, when truncating an IIR filter to an FIR filter, the tap number affects quality of the filtered image quite a lot. And it is not that the more taps there are, the better the quality is. We find there exists an optimal value of tap number that may give the best visual quality, because this filter gives highest contrast of the filtered image. In this paper we analyze this effect using majorization theory and find that the image contrast is actually a Schur convex function on filter coefficients. We also propose an effective method to choose the most concentrated filter, which is the filter that has largest Total Coefficient Energy (TCE). This filter is optimal in terms of image contrast. We apply our optimal anti-aliasing filter on conventional pixel based downsampling and two subpixel based downsampling methods including DDSD and DSD. The results show the strength of the optimal filter obtained by our method. Note that this IIR filter truncating method is not restricted to image downsampling, it can also apply on many different situations, as long as truncating an IIR filter is needed.

One may wonder why we do not consider windowing technique when truncating the IIR filters, since windowing is quite commonly used in filter design. We have actually done some experiment with windowing, and get similar results. The contrast difference between filtered image using different filters are slightly smaller, but the same trend holds. Adding windowing technique is not essential, and makes the problem difficult to analyze, thus we have not included the windowing part in the paper.

Although promising results come out, this is a very preliminary work. For example, we only prove for small neighborhood size that $En = c^T Rc$ is Schur convex. For general case we have not proved yet. We also need to prove that En and TCE follow the same trend, which is demonstrated in this paper by experiment only. More work needs to be done to fix those problems and complete this work.

Table 3: TCE values of 6 filters with different tap number.

image no.	ntap	1	2	3	**4**	5	6	7
1	TCE	0.116	0.077	0.184	**0.267**	0.145	0.126	0.172

Table 4: Contrast values of 6 prefiltered and downsampled test images using DDSD, DSD, and PD methods.

image no.	ntap	1	2	3	**4**	5	6	7
1	DDSD	1824	1810	1913	**1983**	1817	1800	1887
	DSD	1833	1817	1926	**2002**	1827	1810	1900
	PD	1855	1835	1958	**2040**	1850	1831	1925
2	DDSD	2732	2685	2838	**3102**	2806	2698	2785
	DSD	2758	2704	2872	**3158**	2841	2725	2817
	PD	2778	2715	2900	**3213**	2872	2747	2847
3	DDSD	3361	3325	3477	**3685**	3388	3303	3423
	DSD	3379	3338	3504	**3726**	3410	3321	3445
	PD	3403	3358	3531	**3766**	3439	3346	3475
4	DDSD	2518	2472	2783	**2979**	2525	2488	2700
	DSD	2547	2495	2836	**3052**	2564	2523	2748
	PD	2609	2548	2942	**3185**	2645	2597	2845
5	DDSD	6329	6286	6570	**6754**	6325	6286	6490
	DSD	6365	6314	6632	**6838**	6368	6323	6540
	PD	6386	6331	6662	**6883**	6396	6350	6579
6	DDSD	1102	1059	1321	**1502**	1134	1093	1252
	DSD	1128	1078	1374	**1573**	1172	1126	1298
	PD	1179	1117	1456	**1682**	1236	1184	1376

Appendix: Proof of $En = c^T Rc$ being Schur convex function on c in 3×3 case

From Lemma 2.8 of [2] we know that En is Schur convex if and only if $\frac{\partial En}{\partial c_{[i]}}$ is decreasing in $i = 1, \ldots, m^2$, where $c_{[i]}$ is the i-th largest element of c. Since we form c by stacking the columns of the 2-D filter, the largest element is the middle element: $c_{[1]} = h(0,0) = c_{(m^2+1)/2}$. Note here the subscripts of $h(i,j)$ and c_k are related as

$$\begin{aligned} k &= (i+n)\cdot m + (j+n+1) \\ i &= (k-1)\%m - n \\ j &= (k-1)/m - n \\ m &= 2n+1 \end{aligned}$$

The second largest elements are the four 4-connected neighbors of the middle element: $h_{-1,0}, h_{0,1}, h_{1,0}, h_{0,-1}$, i.e. c_{2n^2}, c_{2n^2+2n+2}, $c_{2(n+1)^2}$, c_{2n^2+2n}. For the 3×3 neighborhood case, c is a 9×1 vector and satisfies

$$c_5 \quad > \quad c_2 = c_4 = c_6 = c_8 > c_1 = c_3 = c_5 = c_7 = c_9$$

We need to prove $\frac{\partial En}{\partial c_{[i]}} = 2R_{[i]}c$ is decreasing in i, where $R_{[i]}$ is the associated $[i]$-th row of R. For the 3×3 case, we only need to examine whether $\frac{\partial En}{\partial c_5} > \frac{\partial En}{\partial c_6}$ and $\frac{\partial En}{\partial c_6} > \frac{\partial En}{\partial c_7}$ due to the symmetry.

$$\begin{aligned} &\frac{\partial En}{\partial c_5} - \frac{\partial En}{\partial c_6} = 2[R_5 c - R_6 c] \\ &= 2[(c_5 + 4\rho c_2 + 4\rho^{\sqrt{2}} c_1) - (\rho c_5 + (1 + 2\rho^{\sqrt{2}} + \rho^2)c_2 \\ &+(2\rho + 2\rho^{\sqrt{5}})c_1)] \\ &= 2[(1-\rho)(c_5 + \rho c_2 - c_2) + 2(\rho - \rho^{\sqrt{2}})(c_2 - c_1) \\ &+2(\rho^{\sqrt{2}} - \rho^{\sqrt{5}})c_1] \\ &> 0 \\ &\frac{\partial En}{\partial c_6} - \frac{\partial En}{\partial c_7} = 2[R_6 c - R_7 c] \\ &= 2[(\rho - \rho^{\sqrt{2}})(c_5 - c_8) + (1 + \rho^2 - \rho - \rho^{\sqrt{5}})(c_6 - c_7) \\ &+(\rho + \rho^{\sqrt{5}} - \rho^{\sqrt{8}} - \rho^2)c_1 + (\rho^{\sqrt{2}} - \rho^{\sqrt{5}})c_2] \\ &> 0 \end{aligned}$$

where R_i is the i-th row of R. So En is a Schur convex function on c in the 3×3 neighborhood case. For general cases, the proof is similar.

5. REFERENCES

[1] T. Ojalaand, M. Pietikainen, T. Maenpaa, "Multiresolution gray-scale and rotation invariant texture classification with local binary patterns," Pattern Analysis and Machine Intelligence, IEEE Transactions on, vol. 24, pp. 971-987, 2002.

[2] Daniel P. Palomar and Yi Jiang, "MIMO Transceiver Design via Majorization Theory," Foundations and Trends in Communications and Information Theory, Now Publishers, vol. 3, no. 4-5, pp. 331-551, 2006.

[3] Shuyuan Zhu, Siu-Kei Au Yeung, Bing Zeng, "R-D Performance Upper Bound of Transform Coding for 2-D Directional Sources," Signal Processing Letters, IEEE , vol.16, no.10, pp.861-864, Oct. 2009

[4] L. Fang, O. C. Au, Y. Yang, W. Tang, X. Wen, "Subpixel-based image downsampling-some analysis and observation," in Multimedia and Expo, 2009. ICME 2009. IEEE International Conference on, 2009, pp. 1576-1577.

[5] X. Zhang and X. Wu, "Image Interpolation by Adaptive 2-D Autoregressive Modeling and Soft Decision Estimation," Image Processing, IEEE Transactions on, vol. 17, pp. 887-896, 2008.

[6] R. C. Gonzalez and R. E. Woods, Digital image processing. Beijing: Publishing House of Electronics Industry, 2005.

[7] J. C. Platt, "Optimal filtering for patterned displays," Signal Processing Letters, IEEE, vol. 7, pp. 179-181, 2000.

[8] F. Lu, O. C. Au, Y. Yi, T. Weiran, W. Xing, "A new adaptive subpixel-based downsampling scheme using edge detection," in Circuits and Systems, 2009. ISCAS 2009. IEEE International Symposium on, 2009, pp. 3194-3197.

[9] W. Zhou, A. C. Bovik, H. R. Sheikh, E. P. Simoncelli, "Image quality assessment: from error visibility to structural similarity," Image Processing, IEEE Transactions on, vol. 13, pp. 600-612, 2004.